Tribological Design by Molecular Dynamics Simulation – The Influence of Polar Additives on Wall Slip and Bulk Shear

Seyedmajid Mehrnia*, Maximilian Kuhr, and Peter F. Pelz

Chair of Fluid Systems, Technical University of Darmstadt, Darmstadt, Germany

* Corresponding author: Tel.: +49 6151 16-27107; E-mail address: seyedmajid.mehrnia@tu-darmstadt.de

ABSTRACT

This study employed Molecular Dynamics (MD) simulations to examine the tribological impact of polyalkylmethacrylate (PAMA), a polar lubricant additive known for its role as a Viscosity Index (VI) improver, when combined with the non-polar lubricant polyalphaolefin (PAO) 6. Examining the solid-lubricant interface in a confined liquid between iron surfaces with a Couette flow, the research delves into molecular interactions, emphasizing mechanisms governing wall slip for both non-polar and polar molecules. Notably, for non-polar molecules, a singularity in slip length is observed with a molecular-scale gap height resulting in an infinite slip length. However, the addition of polar additives eliminates slip, leading to increased friction. Furthermore, in terms of bulk shear, the introduction of polar additives reduces shear thinning as temperature increases. This dual observation highlights the substantial impact of polar additives on both wall slip behavior and bulk shear properties in the lubricant system.

Keywords: Slip length, Viscosity index improver, Couette flow, PAO 6

1. INTRODUCTION

This paper explores the concept of tribological design through the application of Molecular Dynamics (MD) simulations, with a focus on the influence of polar and non-polar lubricants on wall slip and bulk shear. Using MD simulations, we investigate the behavior of polar additives within the lubricant film, specifically examining their effects on two critical aspects of tribological performance: wall slip and bulk shear.

Wall slip, characterized by the relative motion between the lubricant and solid surfaces, significantly impacts lubrication efficiency and reliability. By studying the molecular interactions at the solid-lubricant interface, we aim to elucidate the mechanisms underlying wall slip and identify strategies to mitigate its occurrence.

Furthermore, it is crucial to analyze the influence of polar additives, such as polyalkylmethacrylate (PAMA), on bulk shear and understand its underlying mechanisms. The presence of these additives can alter the rheological properties of the lubricant film, affecting its ability to sustain load-bearing conditions. Through MD simulations, it investigated the structural and dynamic properties of the lubricant film in the presence of the polar additives, aiming to comprehend their influence on bulk shear and develop insights into optimizing lubricant formulations.

In the investigation of non-polar molecules in lubrication, several studies have explored the phenomenon of wall slip and bulk shear with hydrocarbon oils interacting with metal surfaces [1-5]. For instance, a slip model was proposed for linear hydrocarbon lubricants confined between metal atom surfaces, considering specific surface parameters and shear viscosity [4]. However, this model is limited to ambient temperatures, lacking consideration for the temperature impact on the slip length. In another study, a linear hydrocarbon model with the United-Atoms (UA) model was

employed to simulate iron with Body-Centered Cubic (BCC) lattice sliding walls, utilizing different temperatures for the fluid, though the effects on wall slip were not explicitly addressed [5].
Ewen et al. investigated the impact of surfactant type and coverage on the slip behavior for n-hexadecane liquid, demonstrating that higher slip length corresponds to lower friction [6]. Furthermore, an MD simulation of a hexadecane oil film sheared between two metal surfaces was conducted, exploring the effects of shear rate, film thickness, and surface energy on wall slip [7].
Exploring wall slip and bulk shear phenomena, particularly in the presence of polar lubricant additives, is a captivating yet insufficiently explored aspect in lubrication science. While existing literature provides glimpses into the potential enhancement of slip with specific additives, a comprehensive understanding of variations in slip length and their intricate relationships with polar lubricant additives remains an uncharted domain.
A study [8] investigated how the addition of a friction-modifying substance affects liquid slip, demonstrating a decrease in friction within hydrodynamic contacts. Another investigation [9] explored the impacts of polar Molecules of crude oil in a MD Simulation study, shedding light on their effects on various properties. Additionally, the study delved into the microscopic mechanism of spontaneous imbibition affected by different polarity molecules. The research provided insights into the complex interactions and behaviors of polar molecules within the context of crude oil, contributing to a deeper understanding of their impact on the studied system. In another examination [10], VI improvers were studied, highlighting challenges faced by oil manufacturers but not specifically addressing slip length in hydrocarbon blends.
Before exploring more details about the simulation, it is essential to provide an explanation of the mechanism of the interface system and its crucial parameters. The application of the apparent and real measurements concept proves particularly insightful in the field of MD tribology, providing a valuable framework for understanding the behavior of fluid films between parallel walls. In scenarios where relative sliding occurs with velocity U between the walls separated by distance h the characterization of apparent shear rate $\dot{\gamma}_{\text{app}} = U/h$, and apparent shear stress $\tau_{\text{app}} = \mu\,\dot{\gamma}_{\text{app}}$ as establishes a practical foundation. Notably, the constancy of the real shear stress across the channel height and its equivalence to the wall shear stress ($\tau(z) = \tau_w$) in stationary Couette flow illuminate the prevalence of molecular (viscous) forces in the overall flow field, particularly under conditions of a small Reynolds number. This fundamental understanding underscores the significance of viscous forces in dictating the shear stress distribution, a critical aspect in the study and analysis of tribological phenomena within confined spaces [1,2].
The relationship between bulk shear and wall slip can be expressed through Navier's slip $\tau = k\,u_s$, and Newton's shear $\tau = \mu\,\dot{\gamma}$ equations. These relationships allow us to establish a connection between the slip velocity u_s and the shear rate $\dot{\gamma}$. Specifically, combining Navier's slip equation with Newton's shear equation, we obtain $u_s = \lambda\,\dot{\gamma}$, where λ represents the slip length, cf. Figure 1. This expression highlights the interrelation between slip velocity and shear rate, providing a means to quantify the wall slip based on established tribological principles.
Examining Newton's constitutive equation $\tau = \mu\dot{\gamma}$ for shear and Navier's boundary condition $\tau_{\text{w}} = ku_{\text{s}}$ in the context of phenomenological tribology and rheology proves beneficial. The parameters viscosity μ and friction factor k, or equivalently, slip length:

$$\lambda = \mu/k \tag{1}$$

, are dependent on the shear rate $\dot{\gamma}$, temperature T, and molecular properties, characterized by the (weight-averaged) molecular weight M. Wall slip and bulk shear are function of

$$\text{shear } \mu = \mu(\dot{\gamma}, T, M), \quad \text{slip } \lambda = \lambda(\dot{\gamma}, T, M, \text{solid}). \tag{2}$$

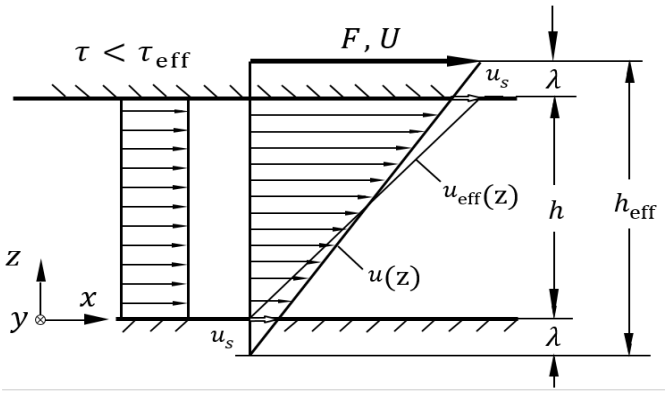

Figure 1: Alteration in the effective gap height caused by the slip length ($h_{\text{eff}} = h + 2\lambda$).

The liquid under investigation in this research is polyalphaolefins (PAO) 6, a base component of synthetic lubricants used in various technical applications. PAO 6 is a hydrocarbon oil primarily composed of branched hydrocarbon molecules, 1-Decane. In addition, Viscosity Index (VI) improvers were used to achieve high-VI hydraulic and gear oils for improved start-up and lubrication at low temperatures. PAMA has long been known in the industry as a key additive to formulate lubricant oils, particularly in the area of green technology-based additives. The structure of 1-Decane tetramer as PAO 6 and PAMA, generated using Avogadro software, are shown in Figure 2.
This paper aimed to extend understanding by exploring Coutte flow under different temperatures, with a particular emphasis on investigating how VI modifiers additves interact with and impact slip and bulk shear mechanisms.

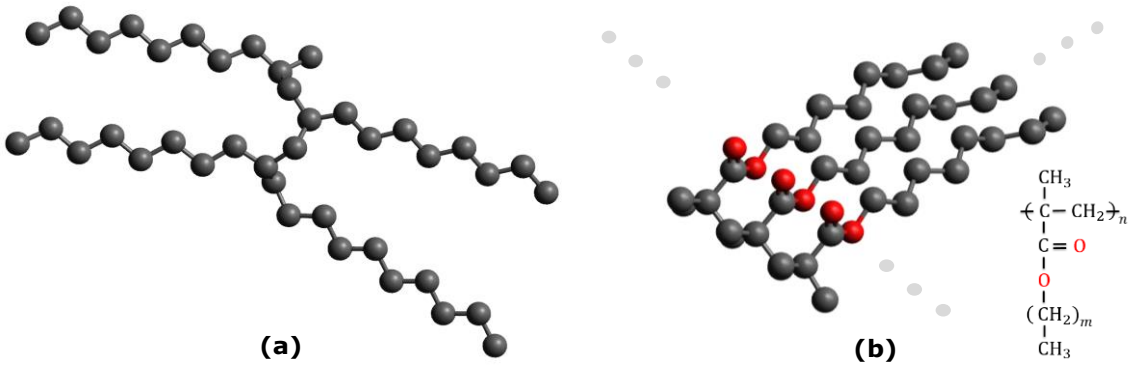

Figure 2: Schematic carbon structures, including (a) a 1-Decane tetramer and (b) a poly alkyl methacrylate (PAMA) comb shape, depicted without their hydrogen atoms.

2. SIMULATION

In this study, MD served as the primary tool for simulating the lubricant-iron system. The classical equation of motion governing a system of atoms was solved to derive the time evolution of the system. To compute the forces within the system, it was imperative to define potential energy functions. The Verlet algorithm, recognized for its precision in simulating atomic motions, was employed as the most accurate numerical scheme in our MD simulation. Additionally, a "neighbor list" numerical scheme was implemented to enhance computational efficiency.

Drawing upon concepts from statistical mechanics, macroscopic considerations were described by classifying microscopic states using an NVE ensemble. To optimize computational time, the United Atom (UA) model was applied specifically to carbon atom groups. Furthermore, a Langevin thermostat was utilized to assist the lubricant atoms in precisely attaining the desired temperature during the simulation.

The Avogadro software was employed for the design of all models, which were subsequently assembled and optimized using the Packmol software. The liquid molecule model adopted in this study incorporates a full atom style, encompassing features such as bond stretching, bending, and torsion. The integration of MD equations of motion utilized the velocity-Verlet algorithm with a time-step of 1.0 fs, specific to the selected force field. The MD simulations were carried out using the open-source LAMMPS molecular dynamics simulator, and a constant NVE integration method was applied to update the velocity and positions of atoms at each time step. The initial macroscopic variables—number of atoms (N), system volume (V), and system energy (E)—were held constant to align with the microcanonical ensemble, ensuring a system trajectory consistent with this ensemble [2,3].

To attain equilibrium, the system underwent relaxation during the initial 0.05 ns of the simulation, ultimately reaching a thermodynamic steady state. Throughout all modeling scenarios, temperature control was uniformly maintained through a Langevin thermostat, mimicking conductive heat flux through the walls to facilitate effective heat removal from the fluid.

Previous research has demonstrated the United Atom (UA) Coarse-Grain models' accuracy in representing hydrocarbon behavior under diverse pressures. The force field selection for MD simulations is critical, and for branched hydrocarbon oil, the NERD-Force-Field was chosen for its applicability to alpha olefins [2]. In the coarse-graining process, CH3, CH2, and CH groups were simplified as single interaction sites. The NERD Force-Field employs an LJ-potential for non-bonded interaction sites, excluding intramolecular interactions within 3 bonds of the same molecule. This non-bonded interaction is characterized by a standard Lennard-Jones 12-6 potential

$$E_{\mathrm{LJ}}(r) = 4\varepsilon \left[\left(\frac{\sigma}{d}\right)^{6} - \left(\frac{\sigma}{d}\right)^{12}\right] \ , \ d < d_c \tag{3}$$

where d is the distance among two pseudo atoms, ε is an energy parameter, σ is specified as the length at which the intermolecular energy within the two pseudo atoms is zero. Thus, it could be called van der Waals radius. ε is the well depth and a measure of attraction between two pseudo atoms. In addition, d_c known as cutoff radius for the LJ-interaction potential is set to 1.15 nm. where the interaction parameters for unlike pairs are calculated through the Lorentz-Berthelot combination rules (Eq. 3 and 4) [3]. Non-bonded LJ potential parameters are tabulated in Table 1.

$$\sigma_{ij} = \frac{\sigma_{ii}+\sigma_{jj}}{2} \tag{4}$$

$$\varepsilon_{ij} = \sqrt{\varepsilon_{ii}\varepsilon_{jj}} \tag{5}$$

Table 1. Non-bonded LJ potential parameters [3].

UA group	ε in meV	σ in Å
CH	3.42	3.85
CH_2	3.95	3.93
CH_3	8.96	3.91
Fe	40.98	2.32

For bond stretching and angle bending interactions harmonic potentials are employed:

$$u_r = \frac{k_r}{2}(r - r_0)^2 \tag{6}$$

$$u_\theta = \frac{k_\theta}{2}(\theta - \theta_0)^2 \tag{7}$$

With r_0 and θ_0 being the equilibrium bond length and angle. The torsional potential is described using the following equation:

$$u_\phi = V_0 + V_1(1 + \cos\phi) + V_2(1 - \cos 2\phi) + V_3(1 + \cos 3\phi) \tag{8}$$

The standard Coulombic interaction potential is employed to describe the charges of atoms in the system. This interaction potential governs the electrostatic forces between charged particles and is fundamental in modeling the interactions between atoms in MD simulations. The Trappe force field was employed for modeling polar atoms in the simulation. All the parameters for the intramolecular potential energy functions can be found in Table 2.

$$u_c(r) = \frac{1}{4\pi\varepsilon_0}\frac{q_i q_j}{r_{ij}} \tag{9}$$

Table 2. Intramolecular potential energy functions parameters [3].

Bond stretching potential	
$k_r = 8.31568\ eV/\text{Å}^2$	$r_0 = 1.54$ Å
Bond bending potential	
$k_\theta = 5.39\ eV/rad^2$	$\theta_0 = 1.99\ rad$
Torsional potential	
CH_x-CH_2-CH_2-CH_y	
$V_0 = 0\ meV$	$V_1 = 31\ meV$
$V_2 = -23\ meV$	$V_3 = 68\ meV$
CH_x-CH_2-CH-CH_y	
$V_0 = 122\ meV$	$V_1 = 34\ meV$
$V_2 = 12\ meV$	$V_3 = -250\ meV$

In the context of simulating the walls, the approach involved the option of using simple spring potentials or opting for a more advanced force field specifically designed for metals. For this simulation, the Embedded-Atom Method (EAM) potential was used to model the iron walls. The EAM is a popular choice for modeling the force field of metals and alloys. It was developed by Daw and Baskes [2] and is based on the density-functional theory for calculating the properties of realistic metal systems. Embedding energy coupled with a pair potential was used to model the bulk material. In studies involving the shearing of hydrocarbon lubricants by molecular dynamics, a common time step employed was 1.0 fs [2].

3. RESULTS

The density distribution depicted in Figure 3 illustrates the distinct molecular layering of three different branched PAO molecules. The regions proximate to the surfaces form an adsorption layer characterized by heightened fluctuations and oscillations in mass density profiles. The observed peak splitting near the surfaces in the mass density profile is significant and can be attributed to the reduced repulsion area of the united-atom (UA) atoms, allowing these pseudo atoms to closely approach the walls and potentially form stronger bonds with the metal atoms. The measured mass density of PAO 6 at ambient temperature is 0.835 g/mL. The average densities of the molecular structures from the MD simulation presented in Figure 3 align with the experimentally measured density.

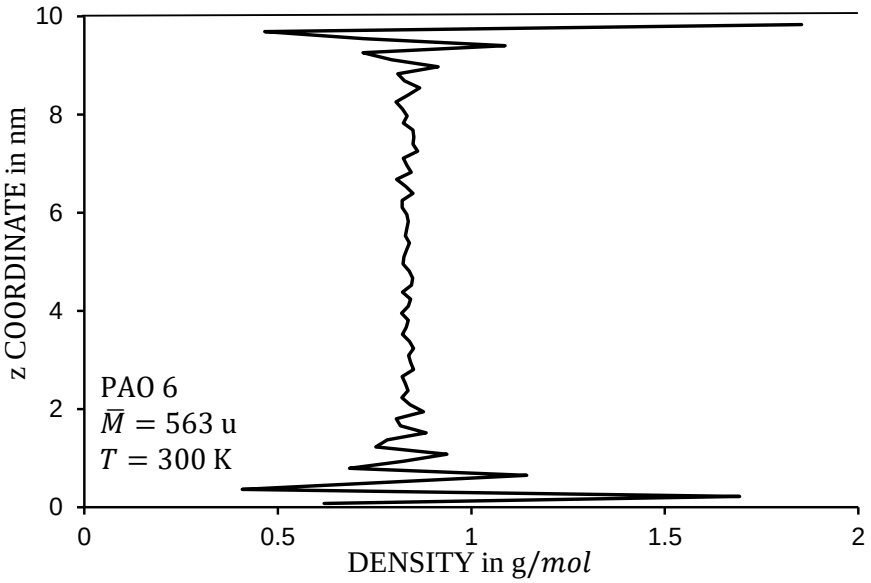

Figure 3: Calculated mass density profile of PAO 6 oil

Contemporary alkene-based lubricants, exemplified by PAO oils, exhibit a dual nature of Newtonian and non-Newtonian behaviors. At low shear rates, viscosity remains constant, forming what is known as the Newtonian plateau. However, beyond a critical shear rate $\dot{\gamma}_c$, there is a swift decrease in viscosity, indicating a shift towards shear-thinning behavior. It's crucial to recognize that the rheological properties of these lubricants are significantly influenced by their molecular structure [14]. Incorporating molecular weight into models, such as the Mark-Houwink relation and the Rouse Model, proves invaluable in establishing a connection between the critical shear rate and the relaxation time of polymeric fluids [15].

Originally designed for short molecules chains, the Rouse model has found applicability in hydraulic fluids, which are characterized by relatively unentangled polymer chains. The model establishes an inverse relationship between critical shear rate $\dot{\gamma}_c$ and the relaxation time r_t of molecules under equilibrium conditions $\dot{\gamma}_c \propto 1/r_t$. Relaxation time is the time for the return of a perturbed system into equilibrium.

The Einstein-Debye equation [11], combined with $\dot{\gamma}_c = 1/r_t$, facilitates the calculation of the relaxation time based on molecular weight and temperature:

$$r_t = \frac{\mu M}{\rho R T} \tag{10}$$

For short-length molecules such as PAO oils, For molecules with short lengths, like PAO oils, both the relaxation time r_t and dynamic viscosity μ exhibit proportionality to molecular weight $\mu \propto M$, $r_t \propto M$. When the product of shear rate and relaxation time is significantly less than 1, $\dot{\gamma} r_t \ll 1$, there is no observable shear rate dependence of shear and slip. In the MD simulation, the relaxation time for the initial Newtonian plateau is determined by the inverse critical shear rate within a 10 ns timeframe, as can be seen in Figure 4. An increase in the number of molecule branches and molecular mass leads to an elevated relaxation time. Additionally, it's noteworthy that higher temperatures result in a higher critical shear rate and, consequently, a shorter relaxation time [2,3].

Figure 4 is shown calculated viscosity profile of PAO 6 oil The fluid's shear viscosity was determined by calculating the ratio of shear stress to the apparent shear rate $\mu = \tau / \dot{\gamma}$ [2]. Utilizing the general equation of the stress tensor for many-body interaction potentials under periodic boundary conditions, the shear stress was computed. In a rheometer, the measured Newtonian viscosity μ_0 of PAO 6 at 300 K was approximately 38 mPa s. Considering that PAO 6 oil is a mixture of different olephins, consist of 1-Decane tetramers, somewhat imprecise comparison can be made.

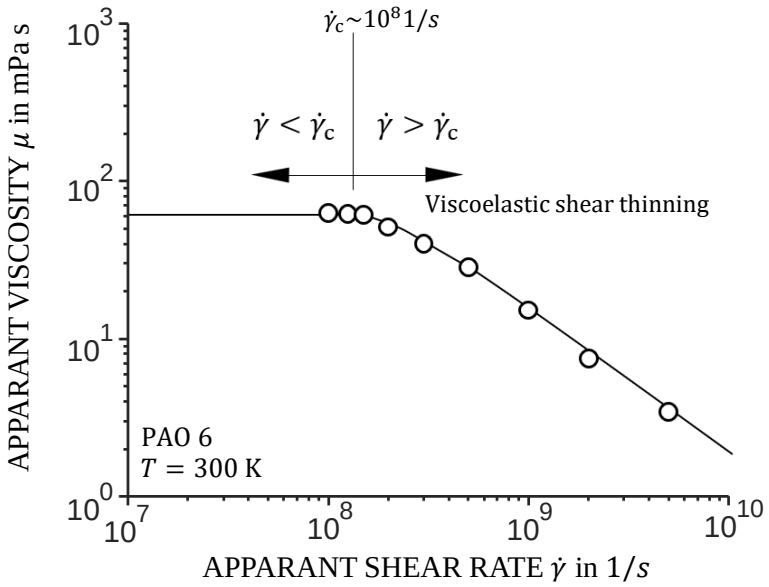

Figure 4: Calculated viscosity profile of PAO 6 oil

3.1. Validation

The accuracy of MD results is closely linked to the force field governing atom interactions, achieving a robust convergence, and the effective implementation of microcanonical ensembles. Additionally, the selection of an appropriate time step for MD simulations plays a crucial role at the simulation's initiation, with the force field determining the requisite time step. Generally, if there is excessive movement among atoms or molecules during two consecutive integrations, the simulation lacks credibility. Table 3 has tabulated a comparison of simulation parameters that shows a good agreement with Ref. [11].

Table 3: Comparison of calculated parameters

Parameter	Ref. [11]	Present work
Density in g/mol	0.832	0.841
Viscosity in mPa.s @ 300 K	38	44
Relaxation time in ns	10.3	9.6

3.2. Wall slip

The relationship between the slip length and the effective molecular length a is evident, as discussed by Pelz et al. [1] through the developed generalized Eyring model for wall slip and Bocquet [12]. This means the slip length scales with the effective molecular length a. It is crucial to emphasize that the assertion $\lambda \sim a$ holds true only under the condition $h \gg a$, an assumption consistently adhered to study by Ref. [1]. However, in cases when $h \sim a$ (length scales in the order of nanometers), the slip length becomes a function of the gap height h as clarified in Figure 5.

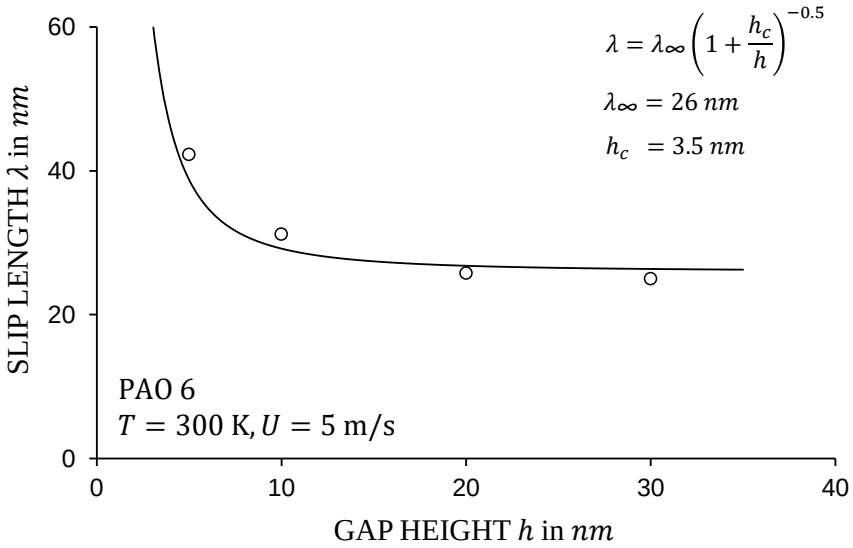

Figure 5: Slip length as a function of gap height when $h \sim a$ for PAO 6 in interaction with iron atoms. As the apparent shear rate is below the critical shear rate, the plotted slip length is independent of the shear rate.

Figure 5 shows the calculated values of slip length λ versus gap heights h and asymptotic expansion Eq. (11) as solid lines. We assumed the critical wall distance $h_c = a = 3.5\ nm$ for PAO molecules. For $h \to 0$ the slip length becomes infinite. This singularity is intuitively understandable, given that for $h \to a$, the slip velocity approaches half of the relative velocity ($w \to U/2$) due to symmetry considerations. The adhesion forces between molecules in the bulk are significantly greater than those between non-polar molecules near the wall and the iron atoms of the wall. Consequently, for $h \to a$, the shear rate approaches zero, resulting in $\lambda \to \infty$.

For $h \to \infty$ we expect a constant value of the slip length $\lambda \to \lambda_\infty$. Hence, an asymptotic expansion reads

$$\lambda = \lambda_\infty \left(1 + \frac{h_c}{h}\right)^{-0.5} \tag{11}$$

This outcome aligns with the findings by Thompson [13], where the functional behavior of λ implies the existence of a universal boundary condition at a solid–liquid interface. When scaling λ by its asymptotic limiting value λ_∞ and shear rate $\dot{\gamma}$ by its critical value $\dot{\gamma}_c$, the data collapses onto an asymptotic relation, described by the equation $\lambda = \lambda_\infty (1 - \dot{\gamma}/\dot{\gamma}_c)^{-0.5}$. The observed behavior suggests that in close proximity to a critical shear rate $\dot{\gamma}_c$, the boundary condition can markedly influence flow behavior at macroscopic distances from the wall, an experimental phenomenon recurrently observed in numerous polymeric systems. This substantial slip is not readily captured by existing phenomenological models. Furthermore, it implies that for flows near $\dot{\gamma}_c$, minor alterations in surface properties can induce significant fluctuations in the apparent boundary condition [13].

In the context of polar additive molecules, their polar functional groups exhibit an affinity for the fluid molecules. This interaction can give rise to a thin layer of fluid molecules in proximity to the surface, commonly referred to as the boundary layer or adsorbed layer. The boundary layer possesses distinct characteristics when compared to the bulk fluid, leading to alterations in viscosity and flow behavior. In this specific scenario, slip values were exceedingly small, approaching zero. This occurs when the fluid molecules strongly bind with the polar molecules, causing them to adhere closely to the surface. Such minimal slip results in heightened friction and increased resistance to flow, leading to reduced flow rates and elevated pressure drop.

Figure 6 shows the presence of a black-marked 1-Decane tetramer molecule situated alongside a metal wall, while being influenced by the presence of polar lubricant additives. This figure provides a side view of the simulation box, depicting a 1-Decane tetramer molecule positioned alongside a stationary surface. Notably, the angle and rotation of the marked black molecule near the stationary

wall are highlighted, offering a comparative analysis between PAO 6 liquid and the blended lubricant PAO 6+VI. The figure vividly illustrates translational rotation in the z-direction, predominantly influenced by the reduced density in close proximity to the stationary wall.
A distinct observation is the molecule's tail flipping while the opposite end remains tethered to the stationary surface. It's noteworthy that the marked black molecule is entangled between polar molecules (oxygen) adhered to the metal surface, adding an additional layer of complexity to the molecular interactions observed in the simulation. This entanglement contributes to the dynamic behavior and rotation of the molecule within the confined space.
As a consequence of this entanglement, there is an increase in friction values, and the slip is observed to be close to zero for the blended lubricant with additives. This phenomenon emphasizes the impact of molecular interactions on the lubrication properties, ultimately influencing the frictional behavior and slip characteristics of the lubricant blend.

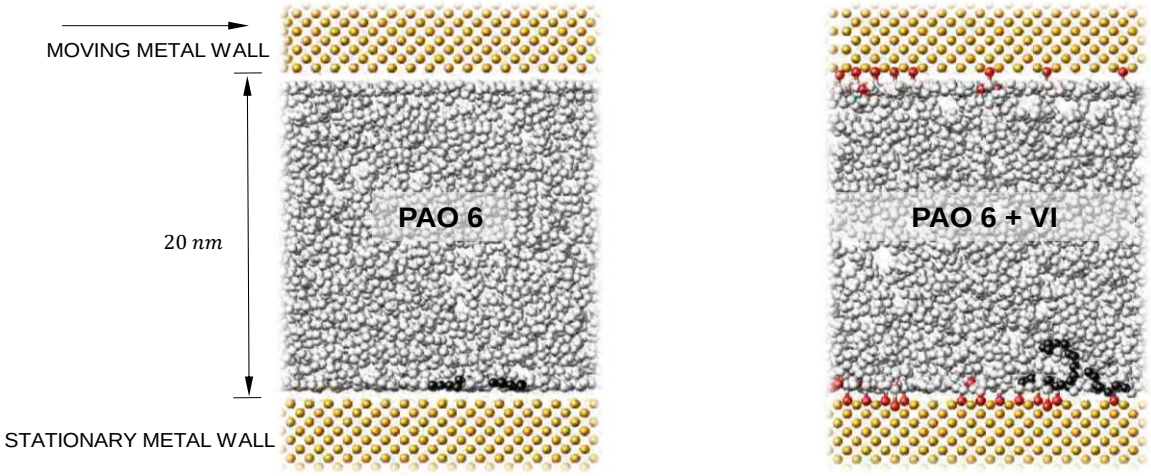

Figure 6: Side view of a 3D simulation box depicting a black marked PAO 6 (1-Decane tetramer) molecule along a metal wall (Fe atoms), with and without PAMA (polar lubricant additives) at 5 ns. Oxygen atoms are highlighted in red, while carbon united group atoms are shown in gray.

3.3. Bulk shear

The presence of PAMA as a VI improver has a significant impact on viscosity, especially at elevated temperatures. The interaction between polar molecules and carbon groups, a characteristic feature of PAMA, plays a crucial role in influencing the viscosity behavior of the lubricant.
To comprehend the role of a VI improver, envision it as a coil spring initially coiled up in a ball at lower temperatures. In this compact configuration, the VI improver has minimal impact on the viscosity of the oil. As temperatures increase, the VI improver exhibits an intriguing behavior— it expands or extends its arms, essentially enlarging its molecular structure. This transformation prevents the oil from thinning out excessively at higher temperatures. The coil spring analogy serves as an effective visualization tool: at low temperatures, the VI improver remains in a condensed state, resembling a coiled spring with minimal influence on oil viscosity. However, as temperatures rise, the VI improver "uncoils," extending its arms to resist excessive thinning of the oil. This property is particularly advantageous in high-temperature environments, as it helps maintain the viscosity of the lubricant within desired limits.

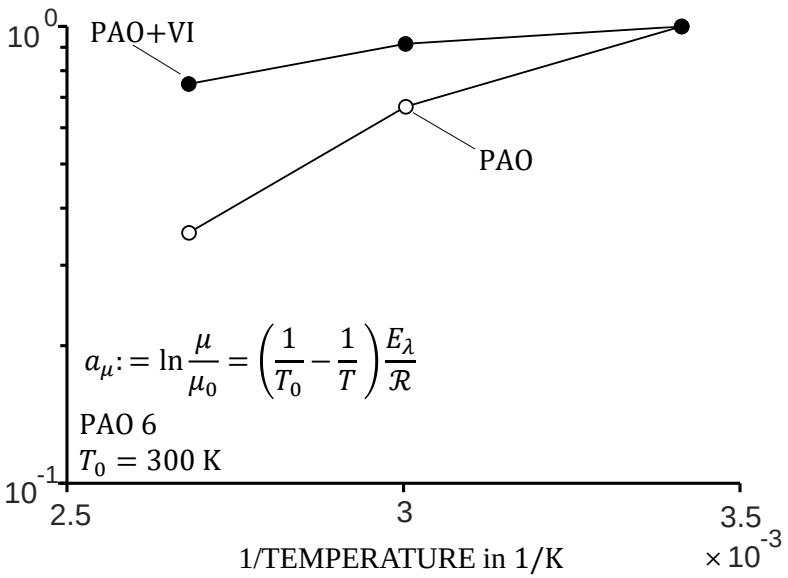

Figure 7: Arrhenius plot of PAO 6 and PAO6+VI to show the effect of polar additive

The Arrhenius plot depicted in Figure 7 provides a visual representation of the impact of incorporating PAMA as a VI additive. This additive plays a crucial role in enhancing the lubricant's viscosity, particularly at elevated temperatures, by dynamically regulating the molecular structure in response to temperature variations. As illustrated in the Arrhenius plot, the viscosity of the lubricant undergoes a notable increase as temperature rises. This is a direct result of the effective action of PAMA as a VI improver. The molecular adjustments facilitated by PAMA prevent excessive thinning of the lubricant at higher temperatures, contributing to enhanced viscosity.

4. CONCLUSION

In the realm of simulations involving confined lubricants, diverse methodologies are employed to assess slip. One such approach entails analyzing the velocity profile of lubricant molecules in proximity to solid surfaces to determine slip velocity. The earlier discussion on singularity in slip length is also touched upon, providing a comprehensive overview of the multifaceted influences in confined lubricant systems. Notably, findings from this analysis indicate minimal slip values, primarily attributed to the presence of polar atoms on wall surfaces. The calculation of viscosity for confined polar lubricant additives combined with PAO oil between metal surfaces in MD simulations demands a consideration of interactions among lubricant additives, PAO oil, and metal surfaces. This involves applying a shear gradient, computing the stress tensor, and analyzing stress autocorrelation to estimate viscosity. The resultant viscosity values underscore the substantial impact of polar molecules on viscosity, chiefly stemming from coil expansion. The concept of coil expansion posits that a polymer maintains a coiled conformation at lower temperatures and subsequently expands as solubility increases at higher temperatures, leading to heightened viscosity. Additionally, the interaction between polar molecules and carbon groups contributes to the increased viscosity observed.

ACKNOWLEDGMENT

We kindly acknowledge the financial support by the German Research Foundation (DFG) within the Collaborative Research Centre (CRC) 1194 "Interaction of Transport and Wetting Processes" - Project-ID 265191195, sub-project C06. The computing time was granted by Lichtenberg HPC computer resources at TU Darmstadt. We appreciate the Hessian Competence Center for High-

Performance Computing – funded by the Hessen State Ministry of Higher Education, Research, and the Arts – for helpful advice.

REFERENCES

[1] Pelz P, Corneli T, Mehrnia S, Kuhr M (2022) Temperature-dependent wall slip of Newtonian lubricants. Journal of Fluid Mechanics 948 A8

[2] Mehrnia S, Pelz P (2021) Slip length of branched hydrocarbon oils confined between iron surfaces. Journal of Molecular Liquids 336 116589

[3] Mehrnia S, Pelz P (2022) Tribological design by Molecular Dynamics simulation– The influence of molecular structure on wall slip and bulk shear. Journal of Chemical Engineering & Technology 46 (1) 95-101

[4] Savio D, Fillot N, Vergne P, Zaccheddu M (2012) A Model for Wall Slip Prediction of Confined n-Alkanes: Effect of Wall-Fluid Interaction Versus Fluid Resistance. Tribology Letters 46 11-22

[5] Ghaffari M, Zhang Y, Xiao S (2017) Molecular dynamics modeling and simulation of lubricant between sliding solids. Journal of Micromechanics and Molecular Physics 2 2

[6] Ewen J, Kannam S, Todd B, Dini D (2018) Slip of Alkanes Confined between Surfactant Monolayers Adsorbed on Solid Surfaces. Langmuir 34 3864-3873

[7] Jabbarzadeh A, Atkinson J, and Tanner R (1999) Wall slip in the molecular dynamics simulation of thin films of hexadecane. Journal of Chemical Physics 110 2612-2620

[8] Choo JH, Forrest AK, Spikes HA (2007) Influence of Organic Friction Modifier on Liquid Slip: A New Mechanism of Organic Friction Modifier Action. Tribology Letters 27 239-244

[9] Wang S, Wang J, Liu H, Liu F (2021) Impacts of Polar Molecules of Crude Oil on Spontaneous Imbibition in Calcite Nanoslit: A Molecular Dynamics Simulation Study. Energy & Fuels 35 (17) 13671-13686

[10] Cusseau P, Vergne P, Martinie L (2020) Relationship between Film Forming Capability and Rheology of Lubricants with VI Improvers. Aus Wissenschaft und Forschung / TAE-Plenarvorträge

[11] Liu P, Lu J, Yu H, Ren N (2017) Lubricant shear thinning behavior correlated with variation of radius of gyration via molecular dynamics simulations. J. Chem. Phys. 147 084904

[12] Bocquet L, Barrat J-L (2007) Flow boundary conditions from nano- to micro-scales. Soft Matter 1235 3(6) 685

[13] Thompson P, Troian S (1997) A general boundary condition for liquid flow at solid surfaces. Nature 389 360-362